A Hybrid Approach to Fabricated Nanowire-Nanoparticle Composites of a Co-W Alloy and Au Nanoparticles

E. Vernickaite,[a] U. Bubniene,[a] H. Cesiulis,[a] A. Ramanavicius,[a,b] and E. J. Podlaha[c,*,z]

[a]*Department of Physical Chemistry, Vilnius University, Vilnius LT-03225, Lithuania*
[b]*Laboratory of BioNanoTechnology, State Research Institute Center for Physical Sciences and Technology, LT-01108 Vilnius, Lithuania*
[c]*Department of Chemical Engineering, Northeastern University, Boston, Massachusetts 02115, USA*

Co-W nanowires were fabricated by pulsed electrodeposition from a citrate-glycine electrolyte onto rotating cylinder electrodes and into nanoporous polycarbonate membranes. The characterization of the electrodeposition conditions and alloy composition of electrodeposited Co-W alloy thin films were determined and used to guide conditions to electrodeposit the nanowires. Gold nanoparticles of 50 nm size were also added to the electrolyte and deposited during electrodeposition of the Co-W alloy nanowires, embedded within, and attached to the nanowire tip, introducing a novel procedure to attached nanoparticles onto nanowires.

Manuscript submitted March 10, 2016; revised manuscript received April 22, 2016. Published May 7, 2016.

Nano-electrodes can be used for various sensing applications, and they can be easily integrated in micro- and nano-scale devices.[1] The sensitivity of nano-electrodes depends on the diameter of electrode tip, and the highest sensitivity is observed by most electrochemical methods if the diameter of the working electrode tip is on the same order of the molecular species being detected. To this end, nano-gaping technology has been applied for the fabrication of nano-electrodes that are based on FIB and E-beam lithographic approaches,[2,3] including electrodeposition and/or chemical etching techniques.[4]

Gold-based 1D nanostructures (e.g., nanowires, gold nanoparticles) have been recognized as unique materials for electrical and optical sensing applications.[5] Gold nanowires can provide high current densities, high signal to noise ratio and low double layer capacitance,[6] while surface plasmon resonance, often exploited with nanoparticles, can uniquely probe interactions of molecules at chemical surfaces and provide label-free bio detection.[5–8]

Gold nanoparticles (AuNPs) are excellent materials for functionalizing electrode surfaces.[9,10] Functionalization can be achieved via the use of bi-functional chemical linking agents, mixing with the components of composite electrodes, covalent binding and others. Notably, gold nanoparticles alone have limited applications in sensing unless surface modification is performed. Careful selection and design of ligands strongly influence the sensitivity and selectivity of a sensor.[5,11] Gold nanoparticles can be synthesized by a citrate reduction method pioneered by Turkevich[12] and later advanced by Frens,[13] with a variety of modification's methods.[6,14–18] The nanoparticle morphology is dependent upon chemical nanoparticle synthesis methods.

Linking agents are typically applied in order to bind gold nanoparticles to surfaces of various substrates.[7,14,19–23] Surface chemical modification and functionalization using linkers both are attractive methodologies because of highly active and selective layer formation, strong electrode intersectional binding, and changeable physical properties. However, there are a few important disadvantages if linkers are applied in order to design nano-electrodes: additional materials affect surface conductivity and can reduce it or lead to poor electrical contact, and they can shorten an electrode's applicable potential window by interfering with electrochemical processes.[24] Direct attachment of AuNPs on the nano-electrode without using any linkers may overcome these disadvantages and even improve the electrochemical performance of the electrode due to uninterrupted conductivity throughout the electrode material. Electrodeposition is one of the most versatile, simple, and cost effective fabrication methods of electrochemical formation of structures and it provides a systematic control of the size and morphology of formed structures.

Hence, this research presents a novel approach for the creation of nanometric electrodes with nanoparticles deposited within and on the top of nanowires. This approach combines two processes: synthesis of nanoparticles, then co-deposition of them in an electrodeposited metal matrix. In order to expand the functionality of the resulting composite nanowire structure, the Co-W alloy was selected as the metal matrix to provide the ability to magnetically move the wire, in contrast to gold. Co-W also offers superior corrosion resistance. As thin films, Co-W alloy has been widely studied for its outstanding tribological properties,[25–29] mechanical durability and superior hardness,[30–33] corrosion resistance,[34,35] and magnetic properties.[36–38]

The electrodeposition of tungsten alloys can be performed in citrate, pyrophosphate and/or ammonium ions containing electrolytes,[39] with the use of citrate being the most widespread particularly for Co-W alloys.[40,41] A challenge in depositing Co-W alloys arises due to the inherent hydrogen evolution side reaction. In order to improve the efficiency of the electrodeposition process and the structure of the obtained Co-W deposits organic additives, such as saccharin, thiourea, methacrylate, glycine can be used in the electrolyte.[42] Recently, glycine-based solutions are of interest because it is a non-toxic complexing agent, which stabilizes the pH close to the electrode surface in both alkaline and acidic electrolytes,[43,44] although the side reaction cannot be completely eliminated. Thus, the management of the hydrogen evolution side reaction can be problematic when translating thin film deposition parameters for Co-W alloys to nanometer architectures via templating methods.

The template-assisted method has been employed for the electrodeposition of nanostructures using a variety of templates, such as polycarbonate membranes,[45,46] and anodized aluminum oxides (AAO).[46–49] Although many investigations have focused on single-element, binary and ternary alloy magnetic nanowires such as Ni, Co, Fe-Co, Co-Ni, Ni-Fe and Fe-Co-Ni,[50–56] no reports of electrodeposited Co-W alloy nanowires exists, except those by the coauthors here. In previous work, Co–W and Co–W–P nanowires and nanotubes were fabricated through the use of pulse deposition using nanoporous alumina templates from ammonia–citrate electrolytes[57] and from ammonia-free electrolytes containing citrate and boric acid.[58] The pulse mode facilitated deposition by minimizing the accumulation of hydrogen gas bubbles and the generation of a significant pH gradient that can disturb the deposition of Co-W alloys, as evident in thin film deposition.

Here, not only is there a further improvement in past techniques of electrodepositing Co-W alloy nanowires, from both an ammonia-free and boric acid-free electrolyte, but a novel composite

*Electrochemical Society Member.
[z]E-mail: e.podlaha-murphy@neu.edu

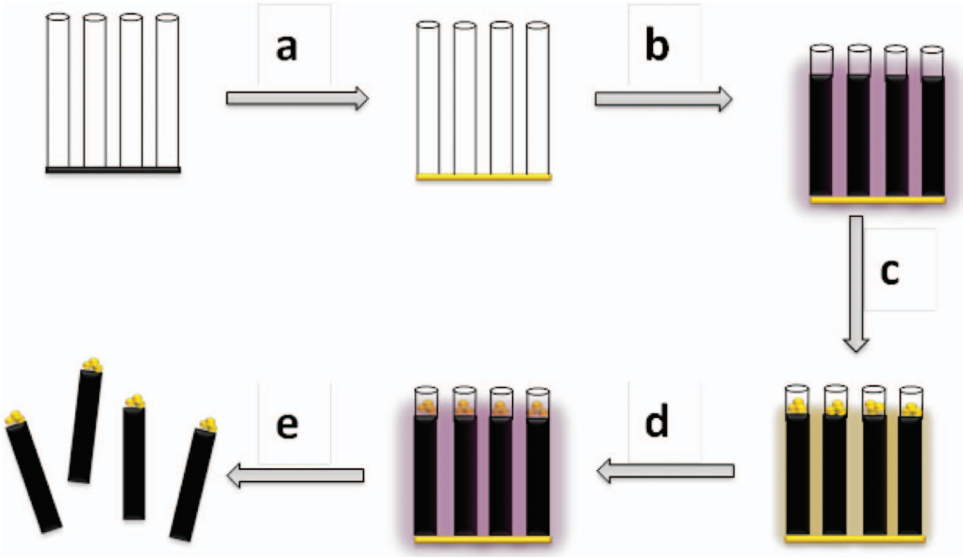

Figure 1. Schematic of the development of nanowire-nanoparticle composites: (a) sputtering a layer of gold; (b) pulsed electrodeposition of Co-W nanowires; (c) adding colloidal gold nanoparticles; (d) pulsed electrodeposition of Co-W alloy; (e) dissolving the membrane.

codeposition approach is presented with nanoparticles deposited on the top of nanowires. The conditions for nanowire deposition were guided by results obtained from polarization curves and galvanostatic, thin film Co-W deposition. In order to avoid mass transport controlled reactions thin, polycarbonate membranes were used as templates compared to previous reports with deeper alumina templates.

Experimental

Co–W thin film alloys and nanowires were fabricated from an electrolyte consisting of: 0.2 M $CoSO_4$, 0.2 M Na_2WO_4, 0.25 M $Na_3C_6H_5O_7$, 0.2 M $C_2H_5NO_2$ and 0.2 M NaOH, at a pH of 10.

The electrodeposition of Co-W thin films was carried out galvanostatically on rotating cylinder brass electrodes (RCE) at 300 rpm under pulsed (PC) and direct current (DC) mode. A platinum anode and a saturated calomel electrode (SCE) were used as the counter and reference electrode, respectively.

Co–W nanowires were electrodeposited into nanoporous polycarbonate membranes using a pulse current mode. Although, past literature reports of pulse parameters have been reported for meso-scale Co-W nanowires,[58] these parameters were selected due to the mass transport considerations inherent to alumina templates, and were optimized for a different electrolyte. With a goal to maintain kinetic control and avoiding gas accumulation and concentration gradients within the pores, thinner polycarbonate films are used here, and a relaxation, or off-time, was chosen to be twice as long as the on-time. Nanoporous polycarbonate membranes with 100 nm pore diameter, 6 μm thickness, having an average porosity of 12% were purchased from Whatman International Ltd. (Whatman Inc., MA, USA). The procedure to fabricate the nanowire-nanoparticle materials is sketched in Fig. 1. In order to provide an electric contact to the membrane a layer of gold was sputtered (Hummer model #Hummer 6.2, Anatech Inc.) on the one side of the templates (Fig. 1a). This Au layer served as a cathode substrate. The Co-W nanowires are formed (Fig. 1b) with an applied cathodic pulsed current density of 80 mA/cm^2 with a 5 s on–time and a 10 s off–time current. After the deposition, the electrolyte was flushed with water. Then the nanoparticle solution was added to the membrane with formed nanowire electrodes and vacuum was applied for 1 minute (Fig. 1c). The nanoparticles were fixed on the surface by deposition of an additional Co-W alloy layer while applying 20 pulses in the same pulse mode as described previously (Fig. 1d). The last step (Fig. 1e) is the release of the wires from the polycarbonate membrane by dissolving the membrane in dichloromethane.

Results and Discussion

The conditions for Co-W electrodeposition were characterized using the RCE at 300 rpm at room temperature. Fig. 2 shows the cathodic polarization curves obtained from −0.4 to −1.8 V vs. SCE in the presence and absence of glycine at pH 10. Addition of glycine to the citrate electrolyte causes an increase in polarization. The cathodic deposition is shifted to more negative potentials due to the expected additional complexation of Co^{2+} and the associated reduction of $CoOH^+$ by the glycine ligand.

Thin film deposition under DC and PC mode was also examined over a range of applied cathodic current densities, 10–80 mA/cm^2 (Fig. 3). The pulse deposition times were: 5 s on-time, t_{on}, and a 10 s off-time, t_{off}. The W content in the alloys electrodeposited under PC mode is slightly higher in comparison with alloys electrodeposited under direct current (DC) mode (Fig. 3a), especially at lower current densities. In both DC and PC modes of deposition the W content is the largest at the low current density and decreases with the applied current density. For DC deposition, there is a limiting amount of the tungsten weight percentage of ∼3 wt% at high current densities. Simultaneously, with a decrease in tungsten content the current efficiency increases sufficiently in both DC and PC modes (Fig. 3b).

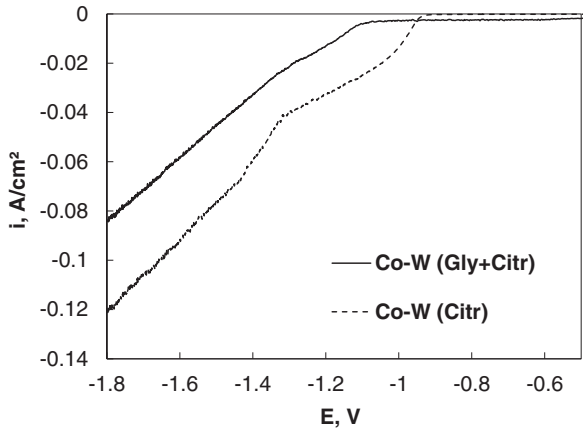

Figure 2. Cathodic polarization curves at 10 mV/s with a RCE at 300 rpm from a citrate bath in the absence and presence of glycine at pH 10, room temperature.

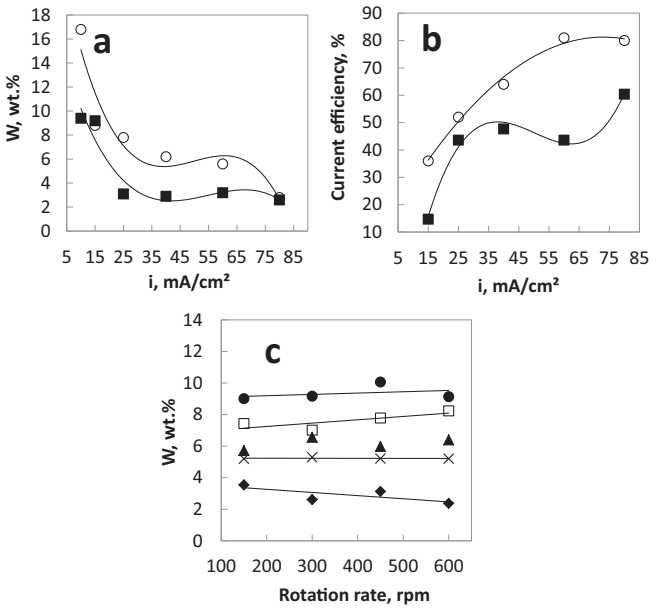

Figure 3. Composition of the Co-W alloys (a) comparing DC (■) and PC (○) deposition; (b) current efficiency; and (c) the influence of the electrode rotation rate under DC plating mode at different current densities: ● 15 mA/cm^2, □ 25 mA/cm^2, ▲ 40 mA/cm^2, ×60 mA/cm^2, ♦ 80 mA/cm^2.

Fig. 3c shows the W wt% for deposition under DC for different applied cathodic current densities at different electrode rotation rates. It is expected, under kinetic control, that the composition would be independent of rotation rate as indeed it is for a cathodic current density of 15–80 mA/cm^2. At higher current densities, a small change in the deposit composition is observed with rotation rate that can signify a mass transport contribution.

The following pulse current conditions were used to form Co-W nanowires within polycarbonate membranes: current density 80 mA/cm^2, pulse on-time of 5 s, and a 10 s off-time. The potential transient during pulse deposition is presented in Fig. 4. The top and bottom of the resulting potential pulse represents the transient in the open circuit potential (OCP) and the deposition potential. Three transient regions were observed in the OCP region, but it is less distinct in the deposition region. The change of slope in the OCP between regions (1) and (2), in Fig. 4, indicates a significant change in either the alloy composition or the surface concentration. During deposition, the potential response is relatively independent with time, confirming little to no mass transport influence of the metal deposition. Thus the changes in regions (1) and (2) during OCP may be reflecting the change in surface pH or adsorbed hydrogen. The last region, (3)

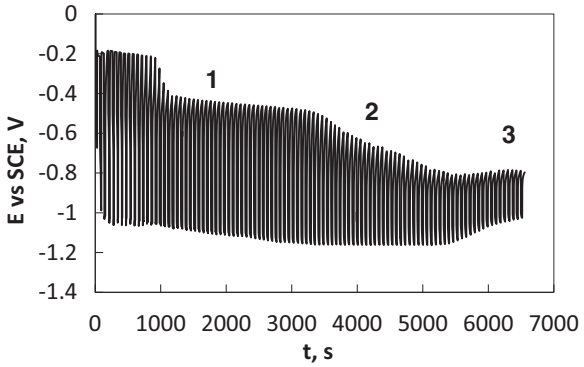

Figure 4. Potential response during PC electrodeposition of Co-W alloy within pores of the membrane.

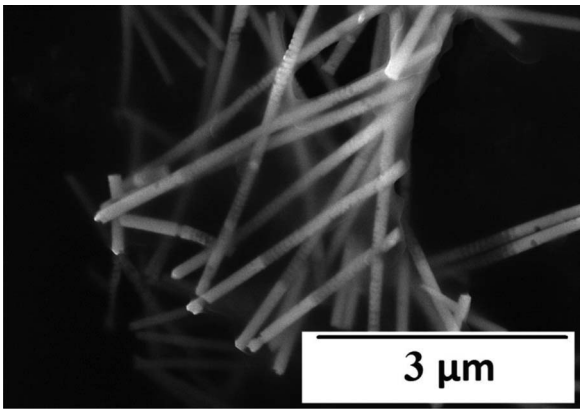

Figure 5. SEM images of electrodeposited Co-W nanowires separated from polycarbonate membranes.

shows the transient response when the nanowires reach the top of the template and commence to grow outside of the pore. The nanowire electrodeposition process was halted at stage (2). After the template was dissolved and the nanowires released SEM (Fig. 5) and TEM images (Fig. 6) confirmed that the long and continuous Co-W nanowires were deposited and their cylindrical shape reflects a complete filling of the nanopores in the radial direction in the template and that they are uniform in diameter. The length of the nanowires matched the expected pore length (6–7 µm). Interestingly, the average diameter of the Co-W nanowires is about 130 nm, which is slightly bigger than the pore size of the PC templates (100 nm).

The composite nanowires, combining the gold nanoparticles with the Co-W matrix, was fabricated using shorter nanowires, (4 µm) created by terminating the deposition process earlier, after 20 min. The Au nanoparticles were placed into the electrolyte, and the deposition process re-commenced to trap them onto the nanowire tip, within the template.

The TEM of the gold nanoparticles (Fig. 7) show that the diameters were fairly uniform having a size of 50 ± 5 nm. Fig. 8 shows that gold nanoparticles were indeed attached to the top of Co-W nanowires. To the best of the authors' knowledge it is the first demonstration of physically attaching nanowires to the end of a metallic nanowire in the form of a composite metal matrix deposit, in contrast to thiol-based chemical attachment.

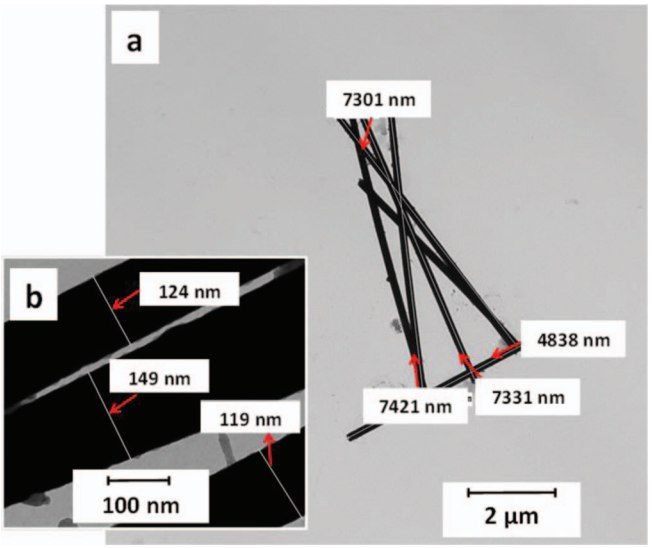

Figure 6. TEM images of Co-W nanowires, (a) low and (b) high magnification with measured wire diameters.

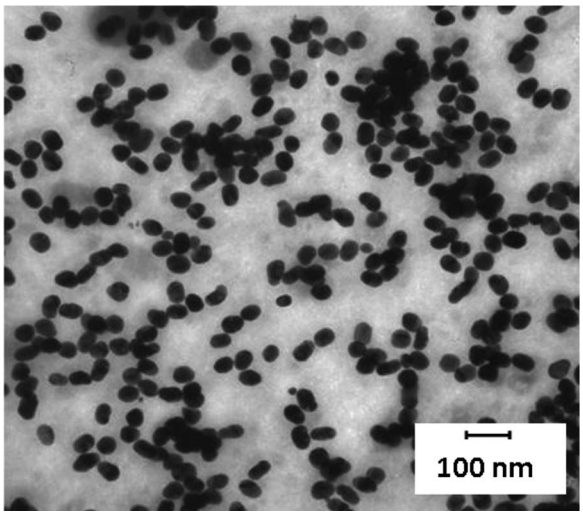

Figure 7. TEM image of 50 nm diameter Au nanoparticles.

Conclusions

Co-W nano-electrodes were fabricated by pulsed electrodeposition from a citrate-glycine electrolyte onto RCEs and into polycarbonate, nanoporous templates having a pore size of 100 nm. Thin film, Co-rich deposits were obtained over a large range of current density, under kinetic control. The addition of gold nanoparticles to the electrolyte enabled the fabrication of unique nano-composite nanowires, composed of Au nanoparticles and a Co-W matrix. The Co-W nanowire and AuNP was chosen as a model system, although the methodology is highly impactful as it could be adapted for other nanowire-nanoparticle complex structures.

Acknowledgments

This work has been funded by the MIP-031/2014 project from the Research Council of Lithuania, European Research Council under European "TEMADEP" (IRSES #05-104-7540), the US National Science Foundation #CHE-0957448, the US National Institutes of Health #1R21hg006278-01. Authors gratefully acknowledge Dr. William Fowle from Department of Biology, EM Lab, NU for help with TEM analyses.

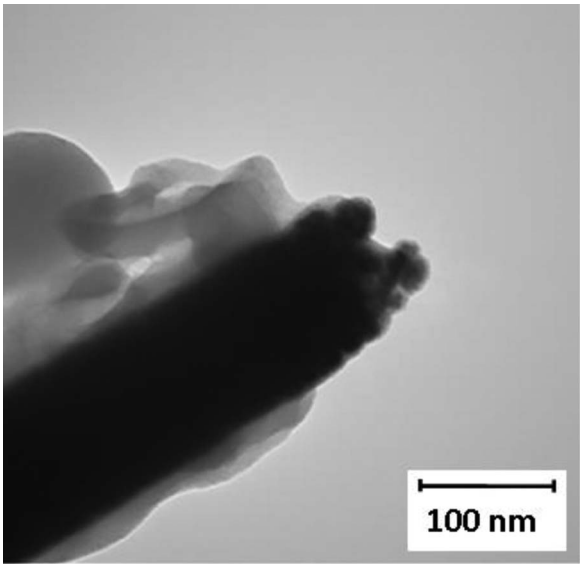

Figure 8. TEM image of Co-W nanowire with Au nanoparticles captured at the nanowire tip.

References

1. J. I. Yeh and H. Shi, *Interdiscip. Rev. Nanomed. Nanobiotechnol.*, **2**, 176 (2010).
2. T. Li, W. Hu, and D. Zhu, *Adv. Mater.*, **22**, 286 (2010).
3. Y. Kashimura, H. Nakashima, K. Furukawa, and K. Torimitsu, *Thin Solid Films*, **438–439**, 317 (2003).
4. X. Chen, Z. Guo, G. M. Yang, J. Li, M. Q. Li, J. H Liu, and X. J. Huang, *Mater. Today*, **13**, 28 (2010).
5. Y. Zhang, W. Chu, A. D. Foroushani, Ho. Wang, D. Li, J. Liu, C. J. Barrow, X. Wang, and W. Yang, *Materials*, **7**, 5169 (2014).
6. A. Akbarzadeh, D. Zare, A. Farhangi, M. R. Mehrabi, D. Norouzian, Sh. Tangestaninejad, M. Moghadam, and N. Bararpour, *Am. J. Applied Sci.*, **6**, 691 (2009).
7. S. T. Sivapalan, B. M. DeVetter, T. K. Yang, M. V. Schulmerich, R. Bhargava, and C. J. Murphy, *J. Phys. Chem. C*, **117**, 10677 (2013).
8. J. Homola, S. S. Yee, and G. Gauglitz, *Sens. Actuators B*, **54**, 3 (1999).
9. F. Li, Y. Feng, P. Dong, and B. Tang, *Biosens. Bioelectron.*, **25**, 2084 (2010).
10. S. Z. Bas, *Mater. Lett.*, **150**, 20 (2015).
11. A. W. Snow and M. G. Ancona, *IEEE Sens. J.*, **14**, 3330 (2014).
12. J. Turkevich, P. C. Stevenson, and J. Hillier, *Discuss. Faraday. Soc.*, **11**, 55 (1951).
13. G. Frens, *Nat. Phys. Sci.*, **241**, 20 (1973).
14. U. Bubniene, M. Oćwieja, B. Bugelyte, Z. Adamczyk, M. Nattich-Rak, J. Voronovic, A. Ramanaviciene, and A. Ramanavicius, *Colloids Surf. A*, **441**, 204 (2014).
15. J. T. Au, G. Craig, V. Longo, P. Zanzonico, M. Mason, Y. Fong, and P. J. Allen, *Am. J. Roentgenol*, **200**, 1347 (2013).
16. C. Li, D. Li, G. Wan, J. Xu, and W. Hou, *Nanoscale Res. Lett.*, **6**, 440 (2011).
17. K. Zabetakis, W. E. Ghann, S. Kumar, and M. Ch. Daniel, *Gold Bull.*, **45**, 203 (2012).
18. M. Sikora, P. Szymczak, D. Thompson, and M. Cieplak, *Nanotechnology*, **22**, 445601 (2011).
19. M. Oyama, A. Orimo, and K. Nouneh, *Electrochim. Acta*, **54**, 5042 (2009).
20. W. Sun, Q. Dai, J. G. Wordena, and Q. Huo, *J. Phys. Chem. B*, **109**, 20854 (2005).
21. F. Patolsky, Y. Weizmann, and I. Willner, *Angew. Chem. Int. Ed.*, **114**, 2429 (2002).
22. M. Urzúa, A. Leiva, F. J. Espinoza-Beltrán, X. Briones, C. Saldías, and M. Pino, *J Nanosci Nanotechnol.*, **12**, 8382 (2012).
23. L. Zhang, X. Jiang, E. Wang, and Sh. Dong, *Biosens. Bioelectron.*, **21**, 337 (2005).
24. J. Zhang and M. Oyama, *Anal. Chim. Acta*, **540**, 299 (2005).
25. S. M. Mayanna, L. Ramesh, B. N. Maruthi, and D. Landolt, *J. Mater. Sci. Lett.*, **16**, 1305 (1997).
26. L. Wang, Y. Gao, T. Xu, and Q. Xue, *Mater. Chem. Phys.*, **99**, 96 (2006).
27. P. Weston, P. H. Shipway, S. J. Harris, and M. K. Cheby, *Wear*, **267**, 934 (2009).
28. H. Capel, P. H. Shipway, and S. J. Hartus, *Wear*, **255**, 917 (2003).
29. N. Tsyntsaru, S. Belevsky, A. Dikusar, and J. P. Celis, *Trans. Inst. Met. Finish*, **86**, 301 (2008).
30. M. Donten, H. Cesiulis, and Z. Stojek, *Electrochim. Acta*, **45**, 3389 (2000).
31. D. P. Weston, S. J. Harris, H. Capel, N. Ahmed, P. H. Shipway, and J. M. Yellup, *Trans. Inst. Met. Finish*, **88**, 47 (2010).
32. T. Yamasaki, *Mater. Phys. Mech.*, **1**, 127 (2000).
33. K. R. Sriraman, S. G. S. Raman, and S. K. Seshadri, *Mater. Sci. Eng. A*, **418**, 303 (2006).
34. R. A. C. Santana, A. R. N. Campos, E. A. Medeiros, A. L. M. Oliveira, L. M. F. Silva, and Sh. Prasat, *J. Mater. Sci.*, **42**, 9137 (2007).
35. Z. A. Hamid, *Mater. Lett.*, **57**, 2558 (2003).
36. H. Chiriac, A. E. Moga, C. Gherasim, and N. Lupu, *Rom. J. Inform. Sci. Technol.*, **11**, 123 (2008).
37. T. Osaka, M. Takai, K. Hayashi, K. Ohashi, M. Saito, and K. Yamada, *Nature*, **392**, 796 (1998).
38. X. Liu, G. Zangari, and M. Shamsuzzoha, *J. Electrochem. Soc.*, **150**, C159 (2003).
39. N. Tsyntsaru, H. Cesiulis, M. Donten, J. Sort, E. Pellicer, and E. J. Podlaha-Murphy, *Surf. Eng. Appl. Electrochem.*, **48**, 491 (2012).
40. Zh. I. Bobanova, V. I. Petrenko, G. F. Volodina, D. Z. Grabko, and A. I. Dikusar, *Surf. Eng. Appl. Electrochem.*, **47**, 493 (2011).
41. N. Tsyntsaru, H. Cesiulis, E. Pellicer, J. P. Celis, and J. Sort, *Electrochim. Acta*, **104**, 94 (2013).
42. G. Wei, H. Ge, X. Zhu, Q. Wu, J. Yu, and B. Wang, *Appl. Surf. Sci.*, **253**, 7461 (2007).
43. O. Ergeneman, K. M. Sivaraman, S. Pané, and E. Pellicer , A. Teleki, A. M. Hirt, M. D. Baró, and B. J. Nelson, *Electrochim. Acta*, **56**, 1399 (2011).
44. M. C. Esteves, P. T. A. Sumodjo, and E. J. Podlaha, *Electrochim. Acta*, **56**, 9082 (2011).
45. S. Dubois, J. Colin, J. L. Duvail, and L. Piraux, *Phys. Rev. B*, **61**, 14315 (2000).
46. S. Aravamudhan, J. Singleton, P. A. Goddard, and S. Bhansali, *J. Phys. D: Appl. Phys.*, **42**, 115008 (2009).
47. I. Z. Rahman, K. M. Razeeb, M. Kamruzzaman, and M. Serantoni, *J. Mater. Process. Technol.*, **153–154**, 811 (2004).
48. A. Saedi and M. Ghorbani, *Mater. Chem. Phys.*, **91**, 417 (2005).
49. Q. Zhan, Z. Chen, D. Xue, F. Li, H. Kunkel, X. Zhou, R. Roshko, and G. Williams, *Phys. Rev. B*, **66**, 134436 (2002).
50. O. Yalçın, G. Kartopu, H. Çetin, A. S. Demiray, and S. Kazan, *J. Magn. Magn. Mater.*, **373**, 207 (2015).
51. B. Hamrakulov, I. S. Kim, M. G. Lee, and B. H. Park, *T. Nonferr. Metal Soc. China*, **19**, s83 (2009).

52. C. Bran, A. P. Espejo, E. M. Palmero, J. Escrig, and M. Vázquez, *J. Magn. Magn. Mater.*, **396**, 327 (2015).
53. A. S. Samardak, F. Nasirpouri, M. Nadi, E. V. Sukovatitsina, A. V. Ognev, L. A. Chebotkevich, and S. V. Komogortsev, *J. Magn. Magn. Mater.*, **383**, 94 (2015).
54. S. Aravamudhan, J. Singleton, P. A. Goddard, and S. Bhansali, *J. Phys. D: Appl. Phys.*, **42**, 115008, (2009).
55. S. Samanifar, M. Almasi Kashi, A. Ramazani, and M. Alikhani, *J. Magn. Magn. Mater.*, **378**, 73 (2015).
56. A. Ramazani, M. Almasi Kashi, M. Alikhani, and S. Erfanifam, *Mater. Chem. Phys.*, **112**, 285 (2008).
57. H. Cesiulis, X. G. Xie, and E. Podlaha-Murphy, *Mater. Sci. Medzg.* **15**, 115 (2009).
58. N. Tsyntsaru, S. Silkin, H. Cesiulis, M. Guerrero, E. Pellicer, and J. Sort, *Electrochim. Acta*, **188**, 589 (2016).